Fracture Response of an Adhesive-Bonded Thermoplastic Composite at Low Temperature

M. Zivkovic, E. Shi, J. Montesano

Composites Research Group, Mechanical and Mechatronics Engineering,
University of Waterloo, Canada

ICCM23 - August 2, 2023

Agenda

- Background
- Introduction
- Sample Preparation
- Experimental Method
- Experimental Results
- Conclusions

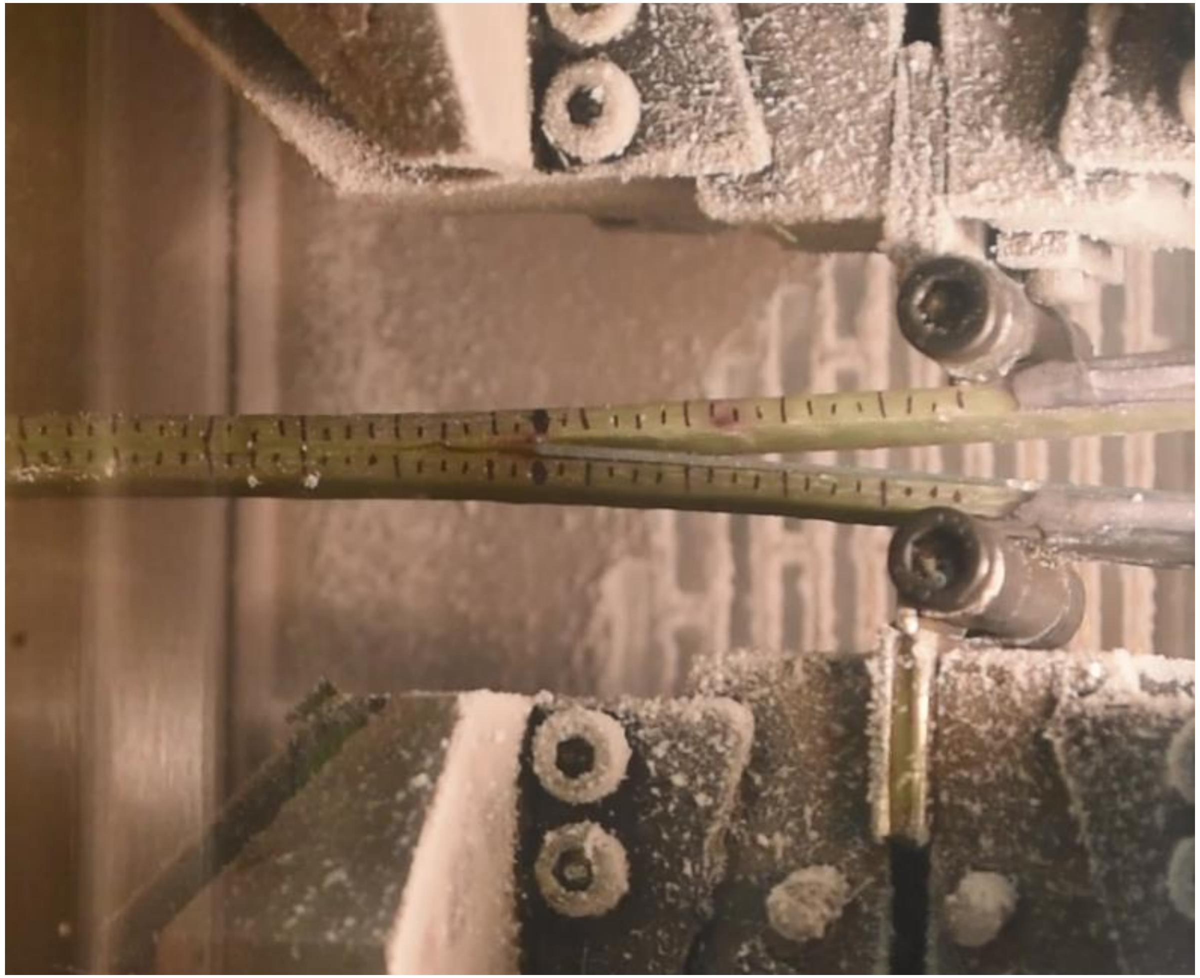

Background – Motivation for Work

- Clean and sustainable energy sources are critical for remote communities
- Micro-generating wind turbines present a viable alternative to diesel generators
- Harsh environments impose a high demand on wind turbine blades

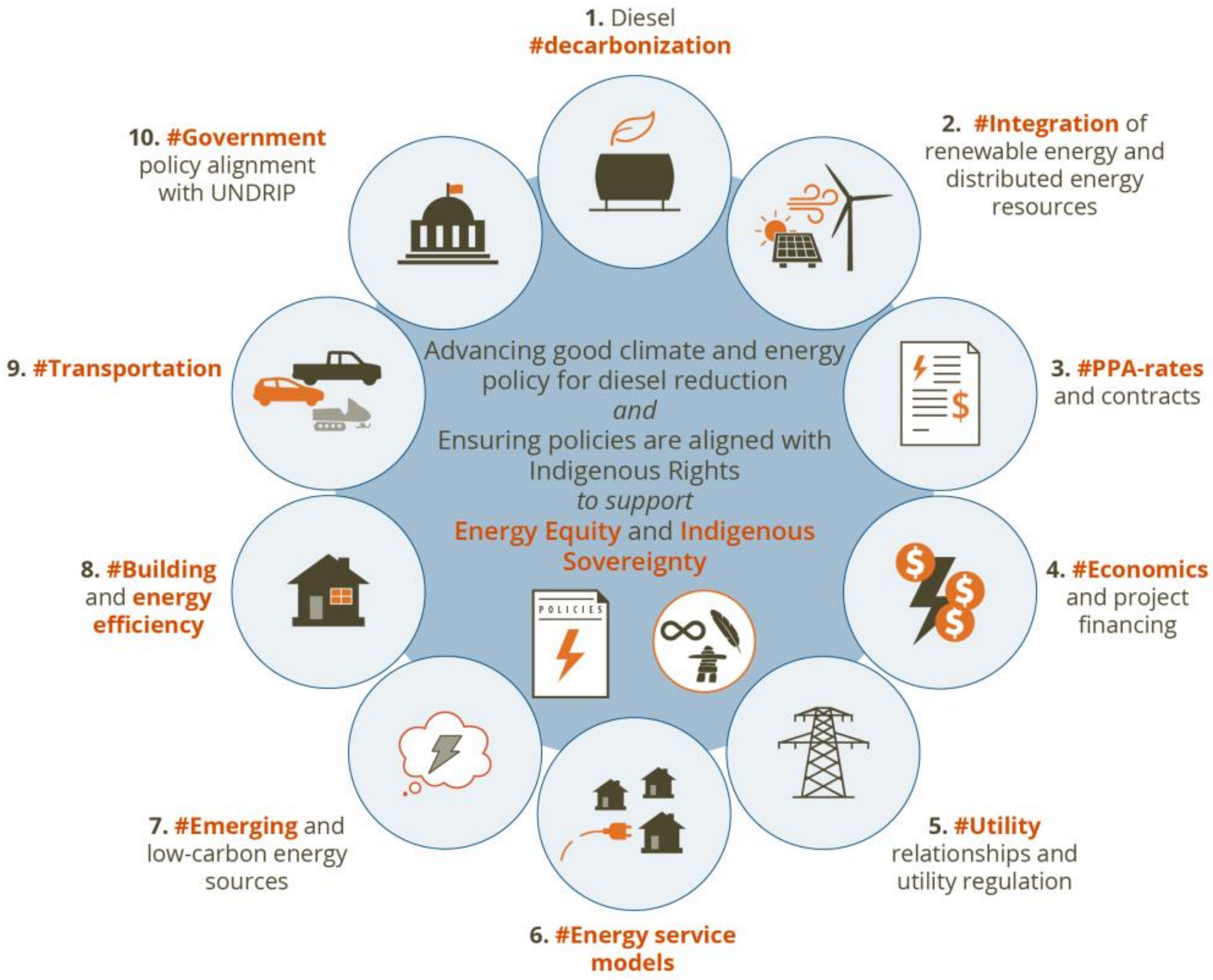

Roadmap for supporting energy projects and promoting diesel reduction in indigenous communities[1].

Background – Turbine Blade Manufacturing

- Our group has developed a resin infusion process for blade shells
- Resin used is a reactive polymethyl methacrylate (PMMA)
- Turbine blade assembly is composed of two adhesively-bonded composite blade shells
- **Thermoplastic composites are more difficult to bond than thermoset composites**

Adhesive-bonded micro-generating wind turbine blade.

Introduction – Thermoplastic Adhesives

- Murray et al. successfully bonded thermoplastic composites with methyl methacrylate (MMA) adhesives[2]
- Thermoplastic adhesive testing with variable temperature has been conducted by Jia et al.[3]
- To the author's knowledge, low temperature testing of methacrylate adhesive with thermoplastic substrate has not been reported

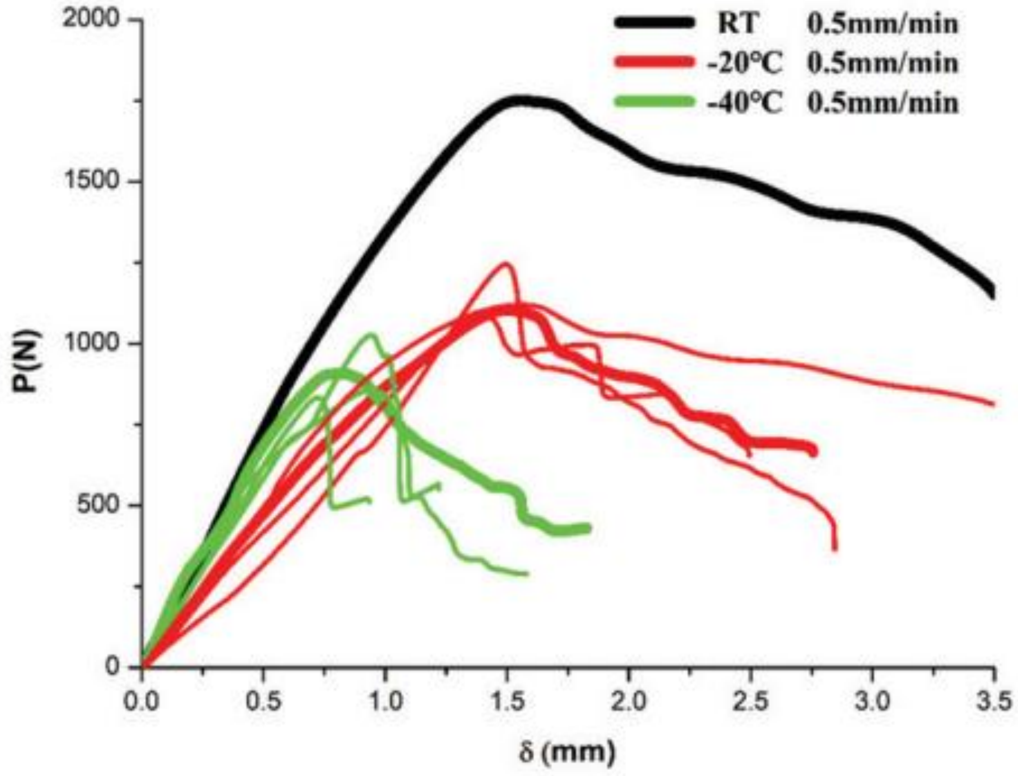

Jia et al. demonstrated that temperature has a drastic effect on polyurethane (thermoplastic) adhesive performance at quasi-static loading conditions[3]. Adhesive used to bond steel substrate.

Objective: Characterizing the temperature and bond-line thickness effect on Mode-I & Mode-II fracture response of a thermoplastic adhesive

Sample Preparation – Substrate

- **Material system**: Elium® 188 XO PMMA resin (Arkema) reinforced with glass fiber unidirectional non-crimp fabric (UD-NCF) (SAERTEX®)
- Substrates underwent abrasion and degreasing surface treatment on mold-side surface prior to bonding
- Substrates bonded with FIT30-45 MMA adhesive (Bostik) with bond-line thicknesses in the range 0.2mm to 1.0mm

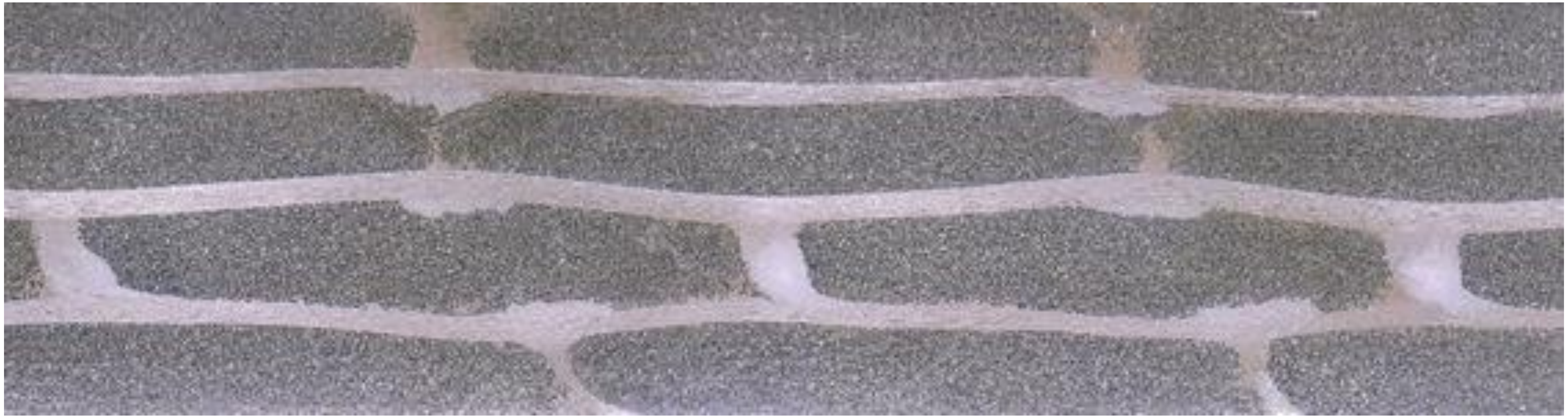

Cross-sectional image of thermoplastic fiberglass panel. $[0]_4$ stacking sequence with ≈48% FVF.

Sample Preparation – DCB Bonding

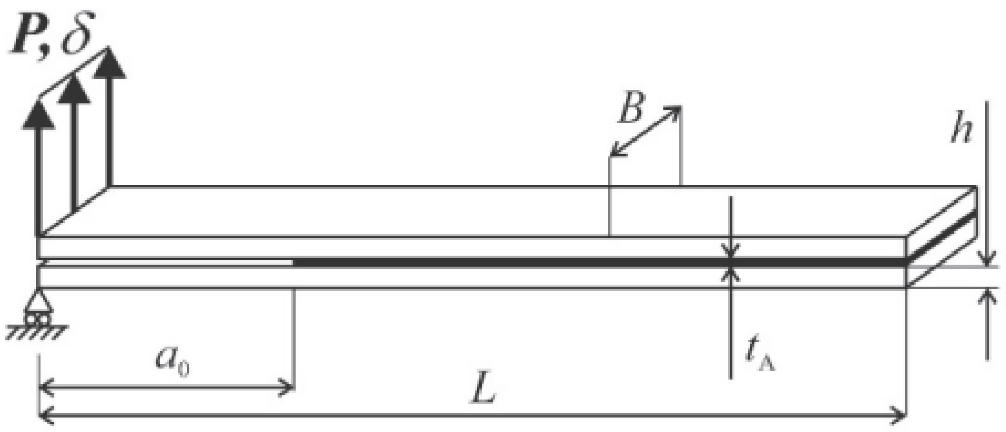

DCB specimen schematic[4].

DCB specimen dimensions.

Shim thickness (mm)	Length L (mm)	Width B (mm)	Bond-line Thickness t_A (mm ±STV)	Pre-Crack; Shim length a_0 (mm ±STV)	Total Sample Thickness $2h$ (mm ±STV)	Average Surface Roughness (µm ±STV)
0.25	140	25.4	0.3268 ±0.04905	45.52 ±0.4417	6.008 ±0.08802	0.764 ±0.0469
0.635			0.7225 ±0.1247	45.41 ±0.4704	6.348 ±0.06547	
0.8			0.8073 ±0.07316	45.89 ±0.4164	6.507 ±0.06178	

Sample Preparation – ENF Bonding

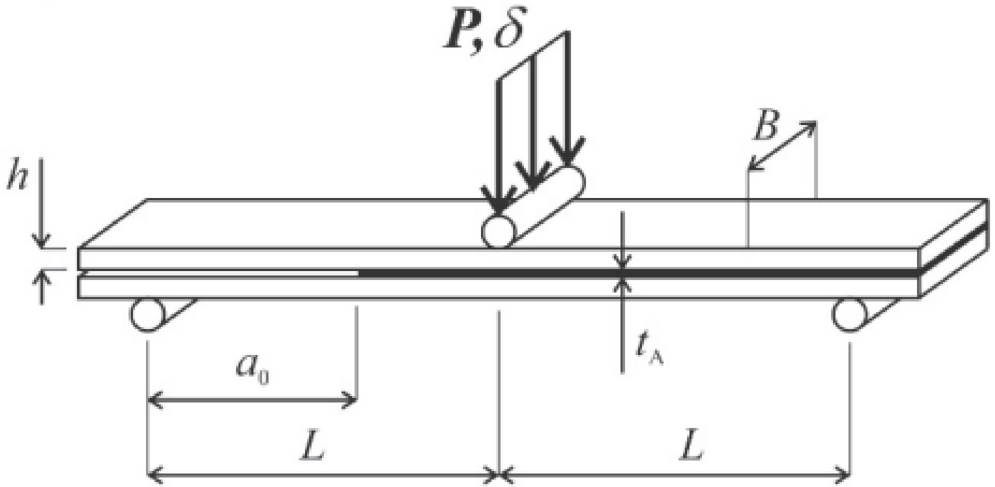

ENF specimen schematic[4].

ENF specimen dimensions.

Shim thickness (mm)	Mid-Span Length *L* (mm)	Width *B* (mm)	Bond-line Thickness t_A (mm ±STV)	Pre-Crack; Shim length a_0 (mm ±STV)	Total Sample Thickness *2h* (mm ±STV)	Average Surface Roughness (µm ±STV)
0.25	75	25.4	0.3041 ±0.04639	51.41 ±0.2635	6.147 ±0.1819	0.764 ±0.0469
0.475			0.6052 ±0.02707	52.68 ±0.5493	6.429 ±0.08791	
0.675			0.7211 ±0.06853	52.46 ±0.3609	6.480 ±0.06961	

Experimental Method – Fixture Setup

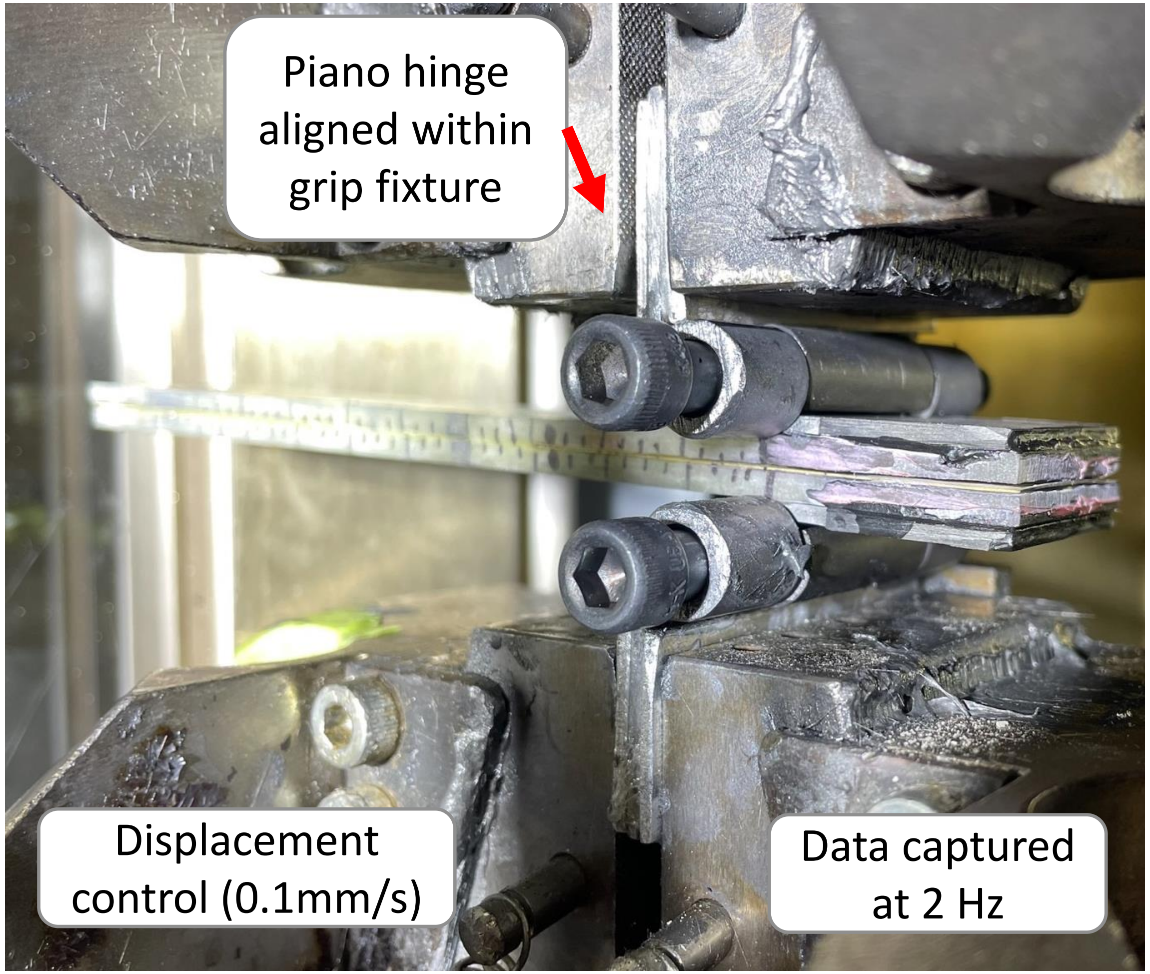

Piano hinge fixture setup for DCB testing.

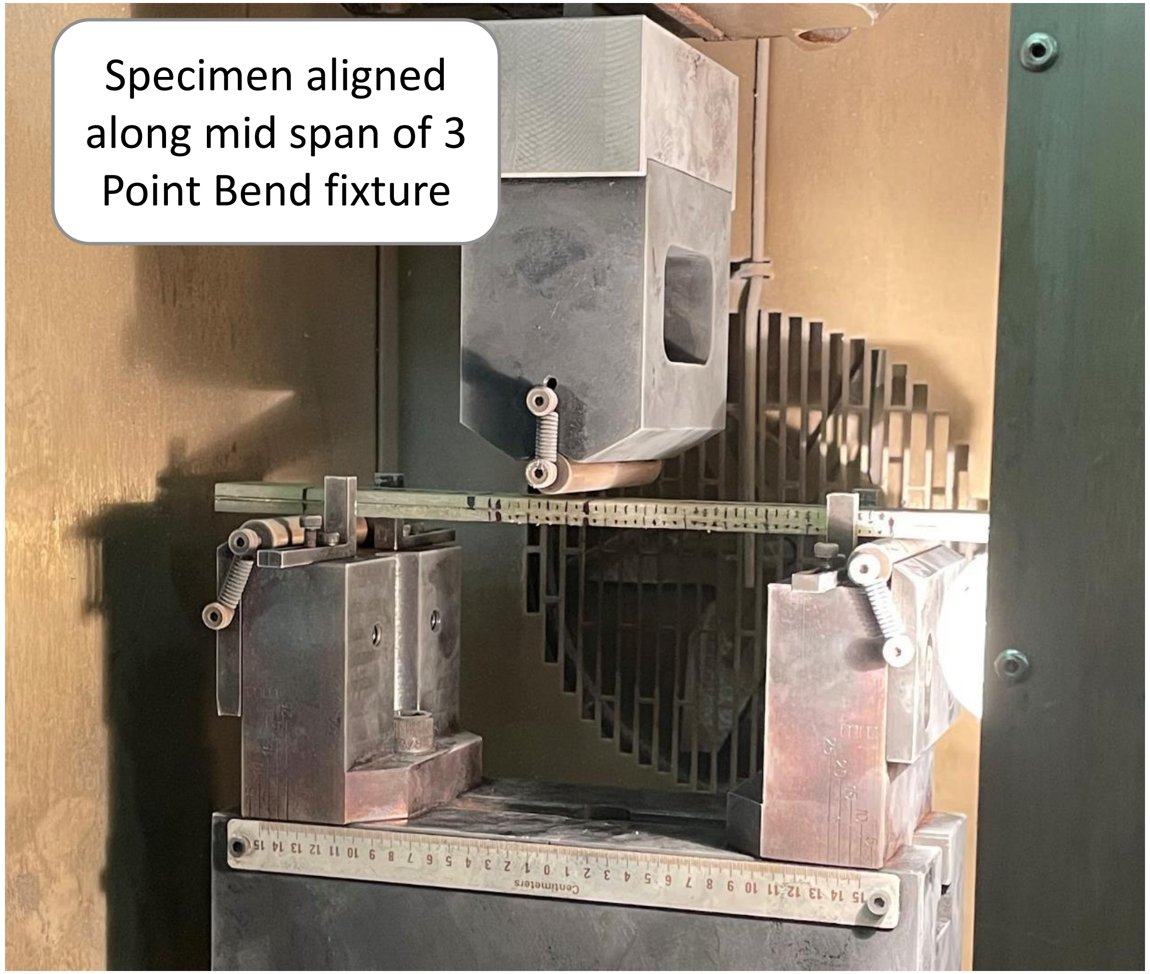

3 Point Bend (3PB) fixture setup for ENF testing.

Experimental Method – LT Test Setup

- Samples tested using MTS 810 servo-hydraulic test frame
- Climate chamber with LN2 canister used for LT tests
- Cooling rate of -6.5°C/minute followed by conditioning for 5 minutes at set temperature of -40°C

LN2 canister used to cool climate chamber for LT tests.

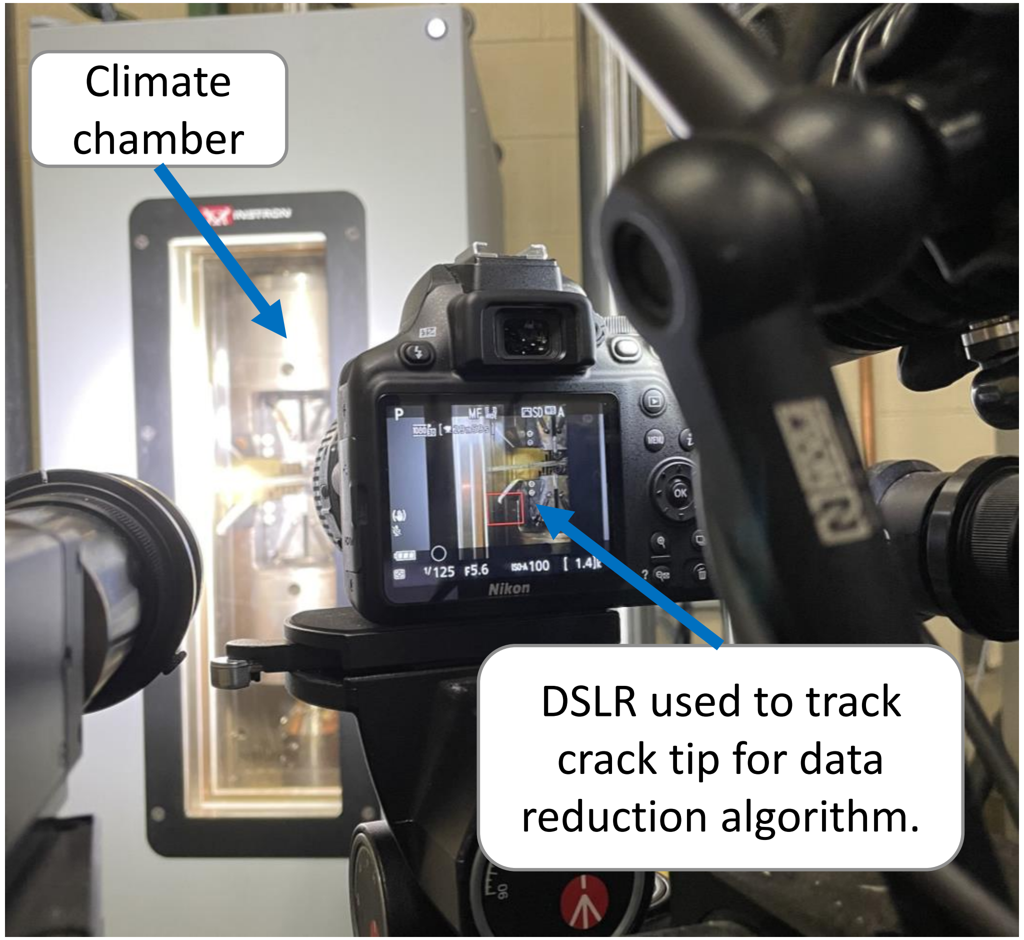

Sample enclosed within climate chamber; crack front still visible through glass with DSLR.

Experimental Results – Mode-I

0.25mm 0.635mm 0.8mm

RT

LT

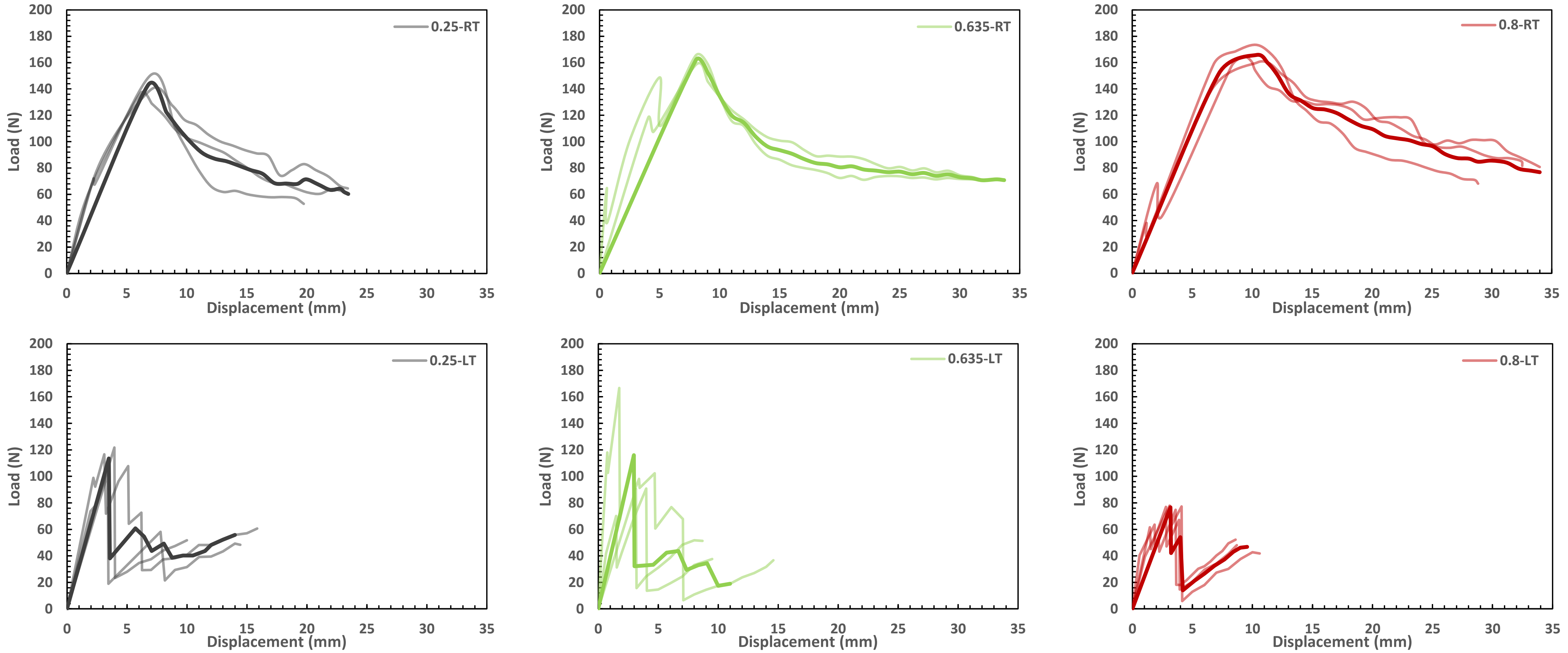

Experimental Results – Mode-I Fracture Toughness

- *Modified Beam Theory (MBT) Method (from ASTM D5528)* used to determine mode-I strain energy release rate (G_{IC})[5] for RT-DCB samples
- LT-DCB G_{IC} calculations incomplete due to errors in elastic curve

Below: G_{IC} calculations using MBT method for RT-DCB specimens.

Bond-line Thickness (mm)	G_{IC} (N/mm)
0.25	0.929
0.635	1.231
0.8	1.632

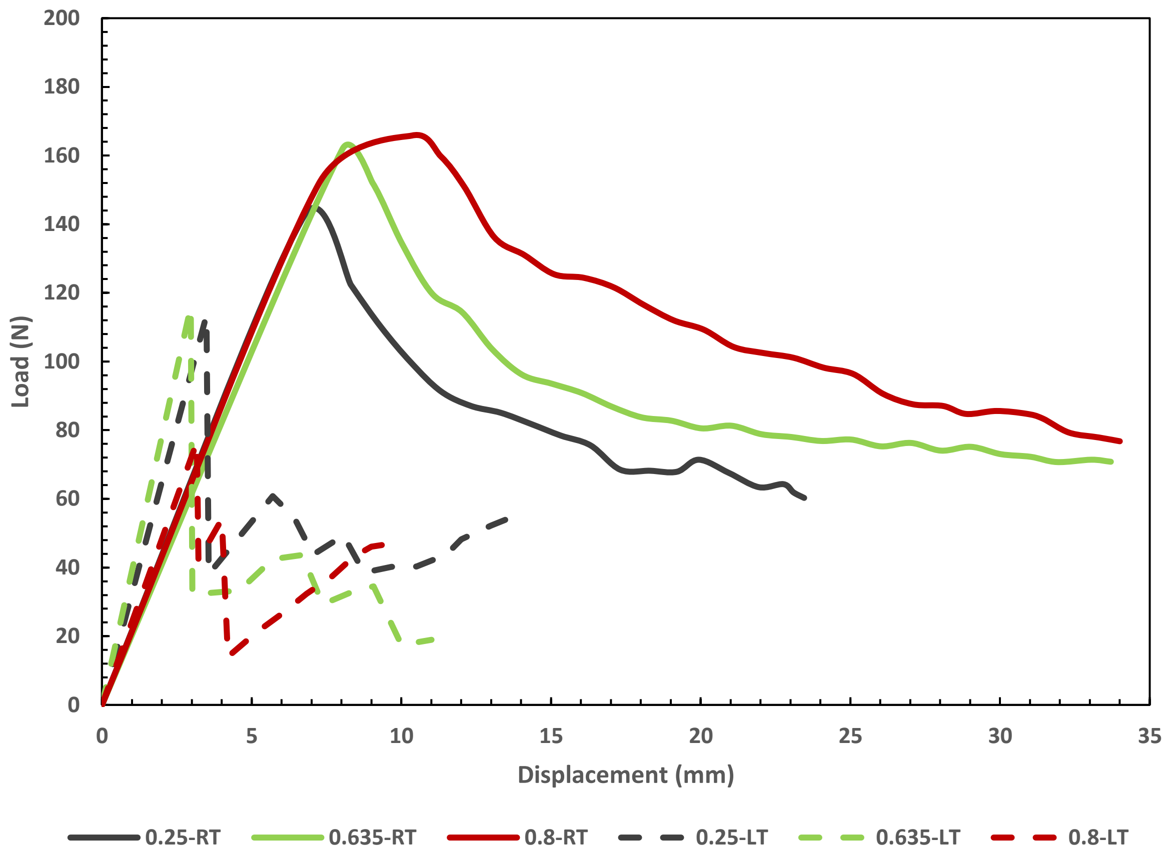

Overlay of average Load-Displacement curves for DCB tests at RT and LT.

Numerical Model – Mode-I RT

- RT-DCB experiments simulated in ABAQUS using cohesive elements to determine TSL parameters
- G_{IC} from experimental results used as fracture energy input
- Discrepancies in elastic response may be due to process errors during sample bonding

Bilinear traction separation law parameters for ABAQUS simulations.

Bond-line Thickness (mm)	Initial Stiffness (MPa)	Peak Traction (MPa)	Fracture Energy (MPa mm)
0.25	1000	15	0.929
0.635	500	15	1.23
0.8	2000	15	1.63

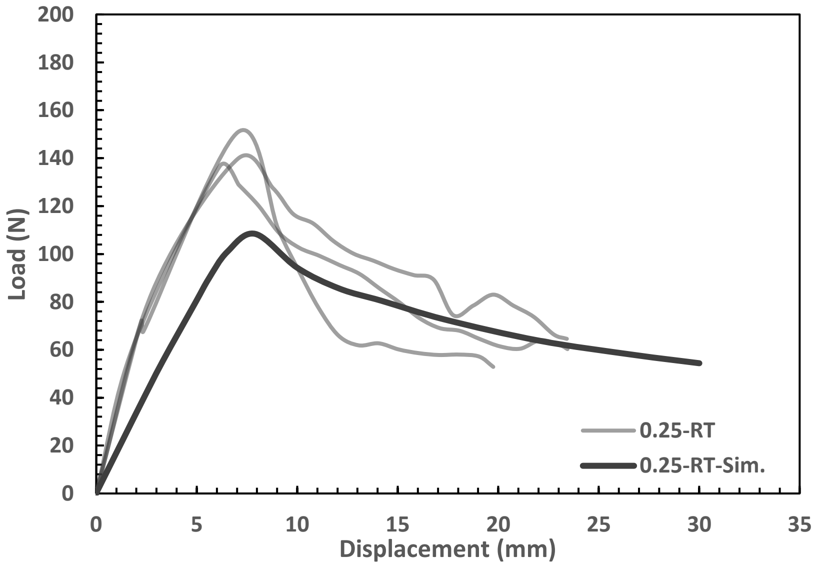

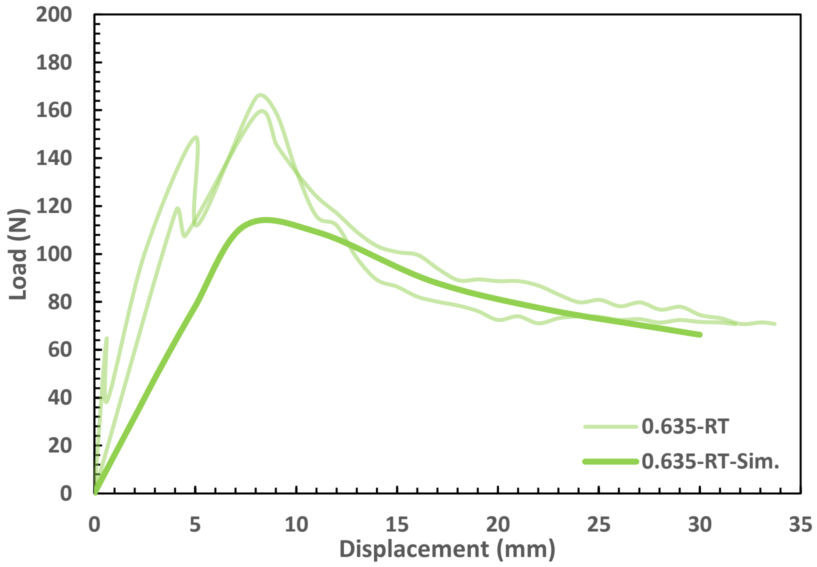

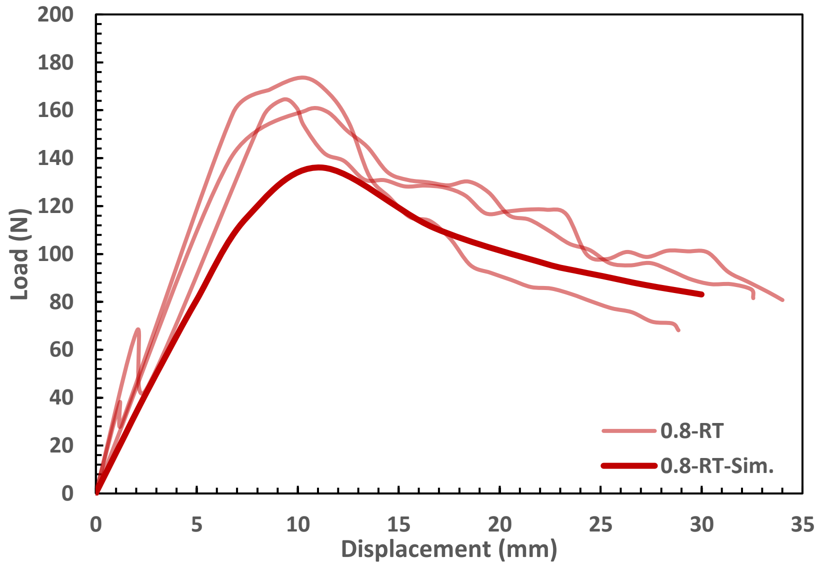

Fracture Analysis – Mode-I RT

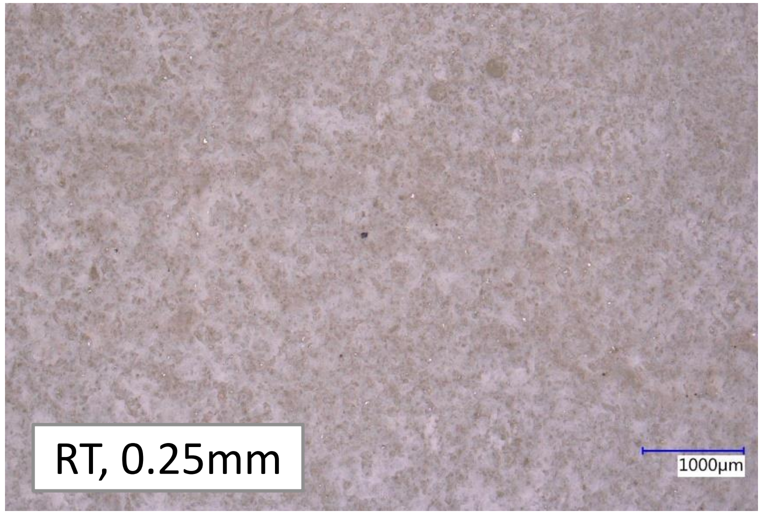

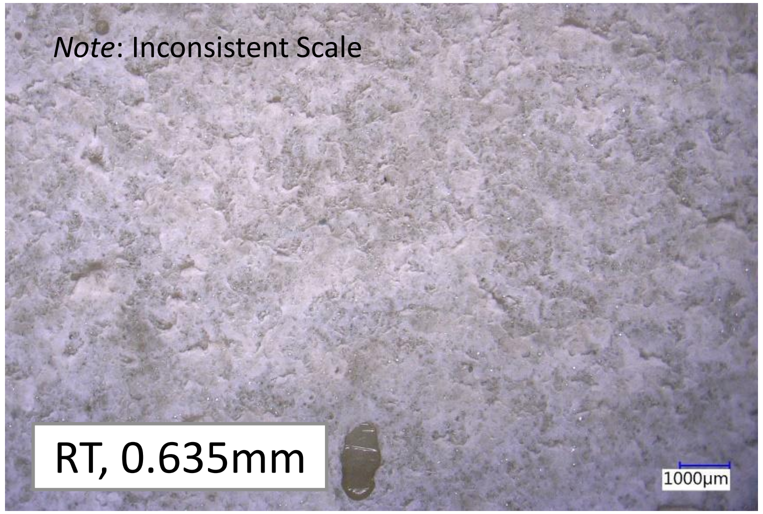

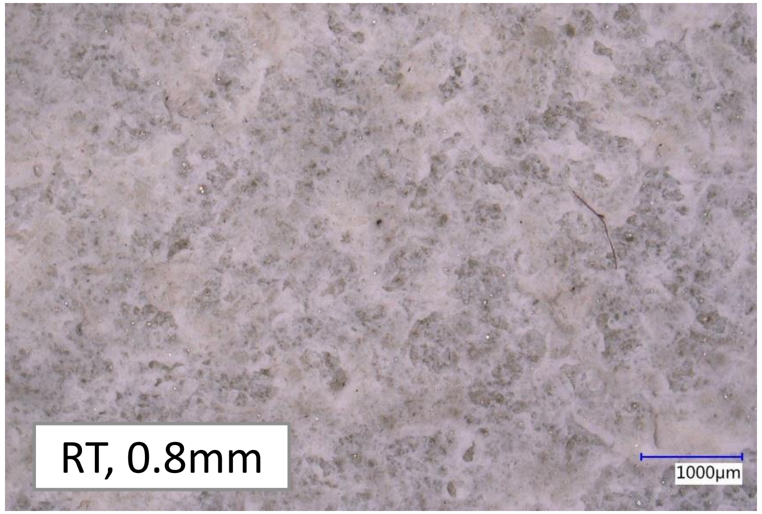

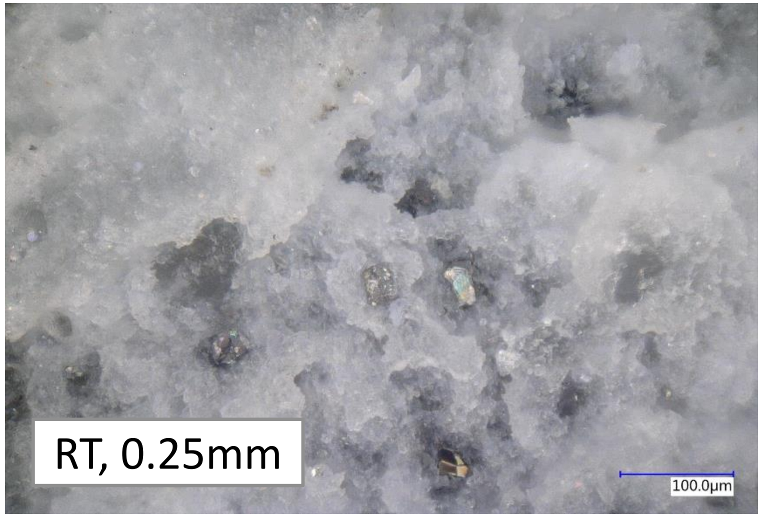

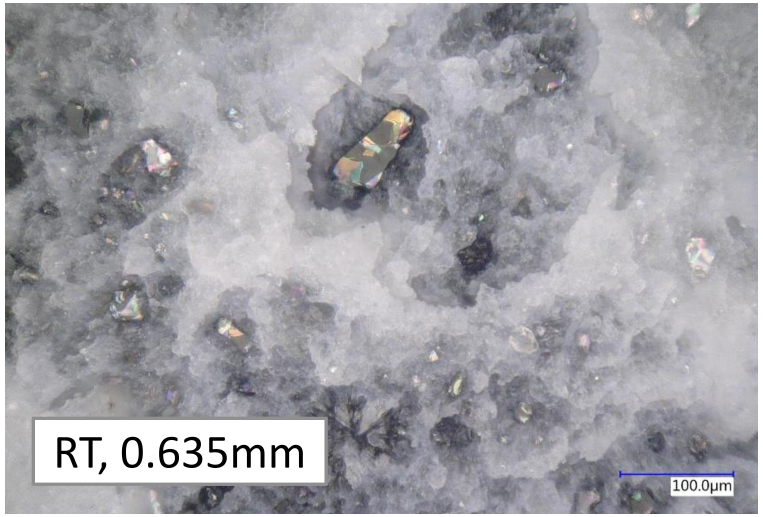

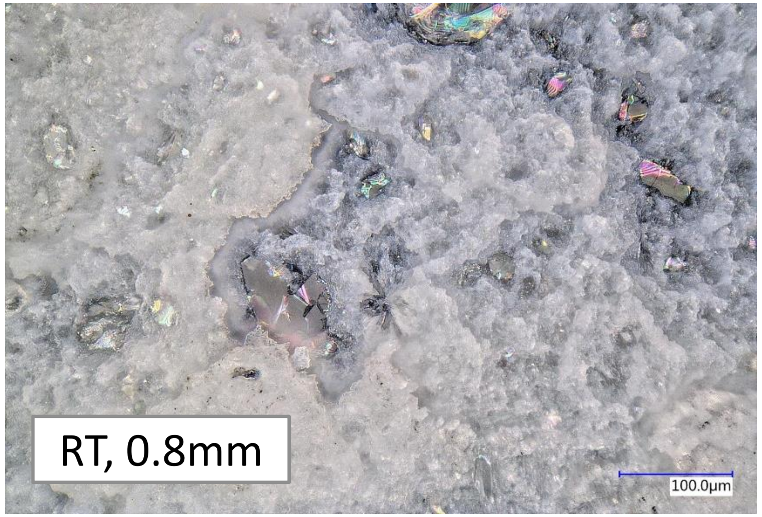

Fracture Analysis – Mode-I LT

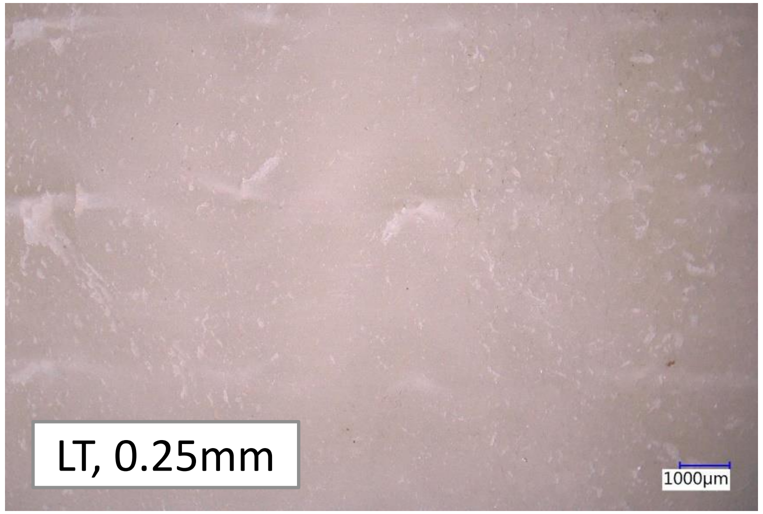

LT fracture surface.

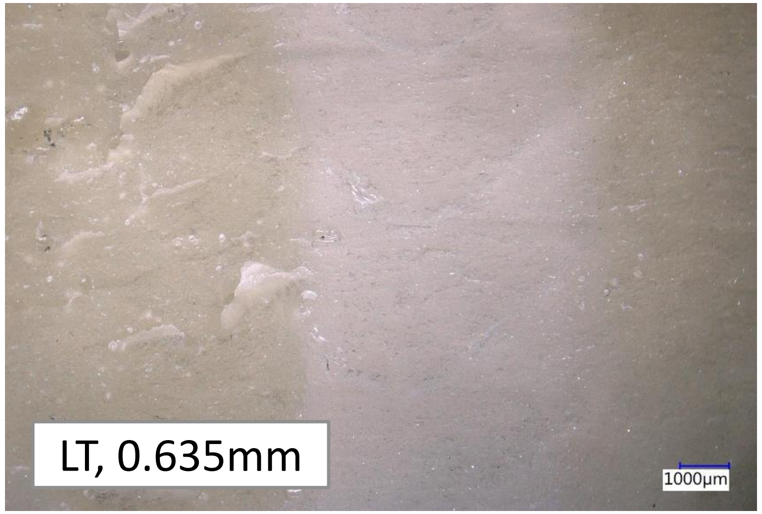

LT fracture ridge/valley.

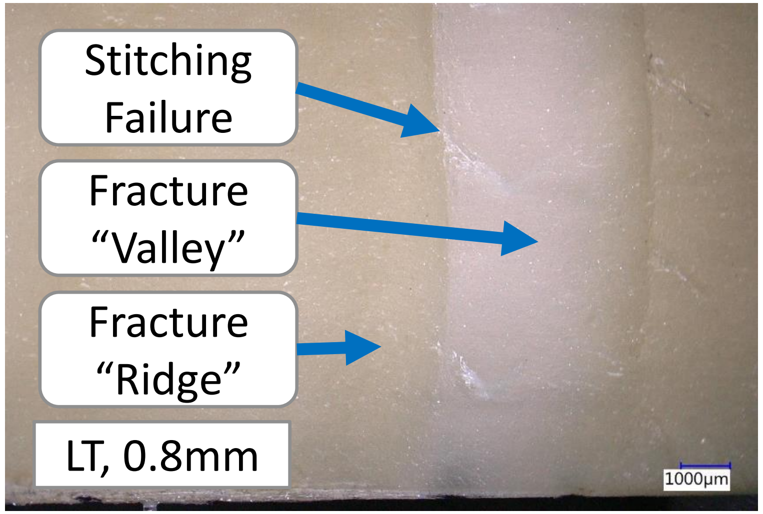

LT fracture ridge/valley with exposed stitching.

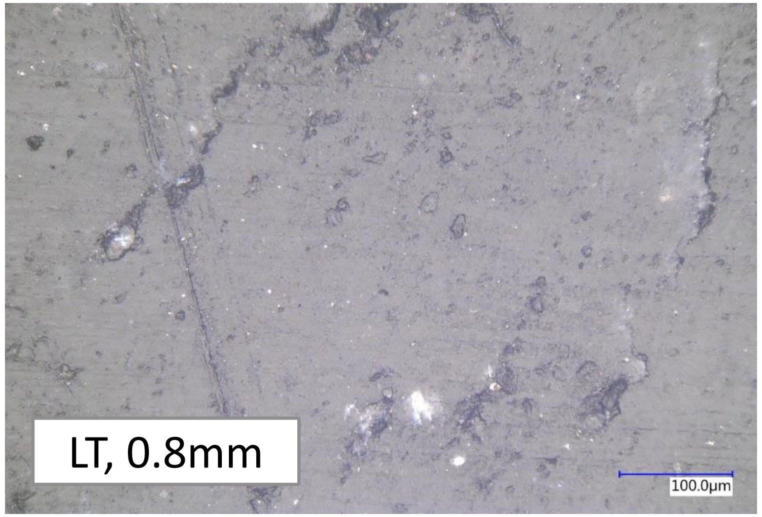

Unbonded composite at 500x magnification.

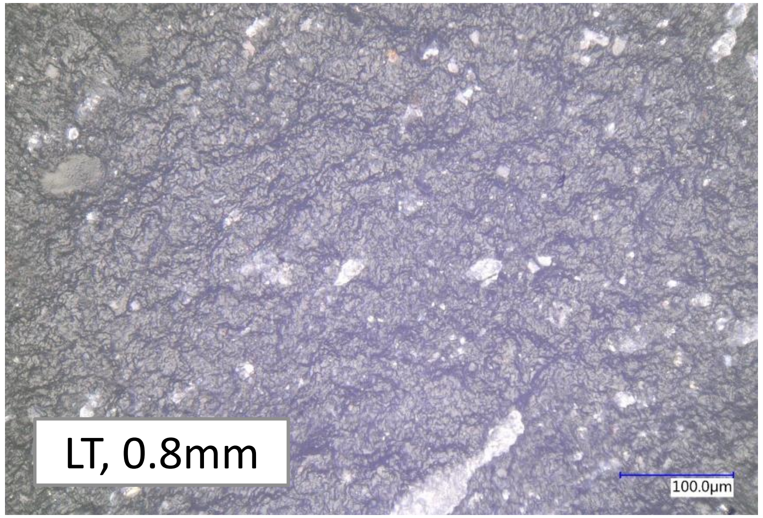

LT fracture ridge at 500x magnification.

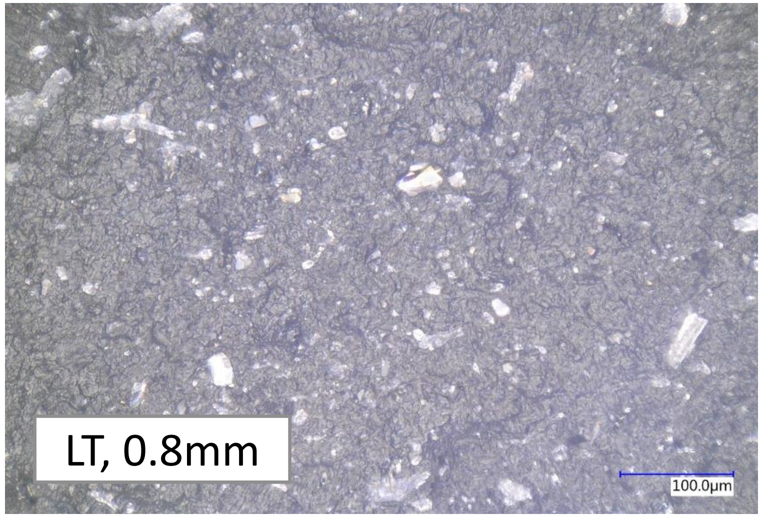

LT fracture valley at 500x magnification.

Fracture Analysis – Mode-I LT

- LT-DCB samples characterized by oscillatory “groove” patterns (valleys and ridges)
- Residual stresses caused by specimen cooling may have increased crack-path instability (T-stress theory)[6]
- 3D depth display was used to characterize surface roughness for varying adhesive thicknesses

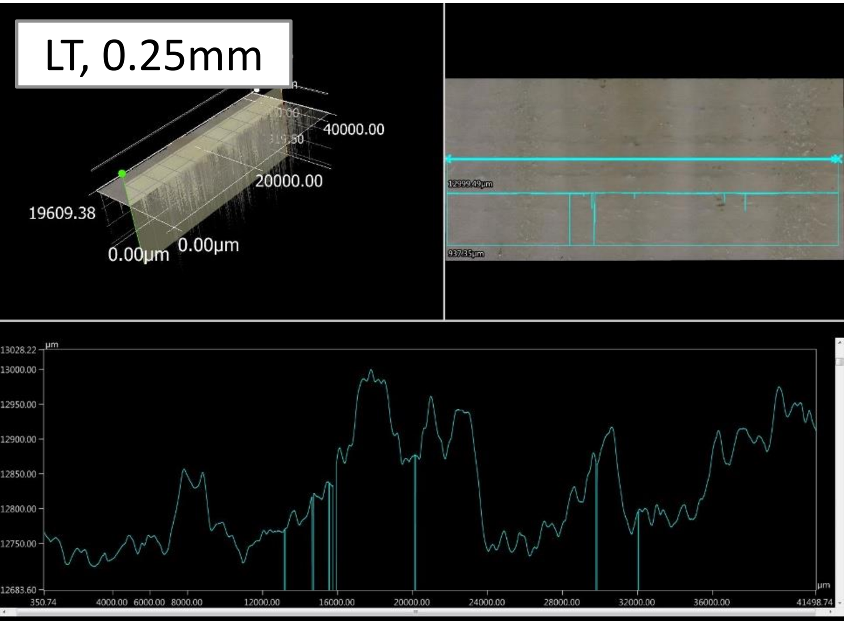

Rz: 201µm

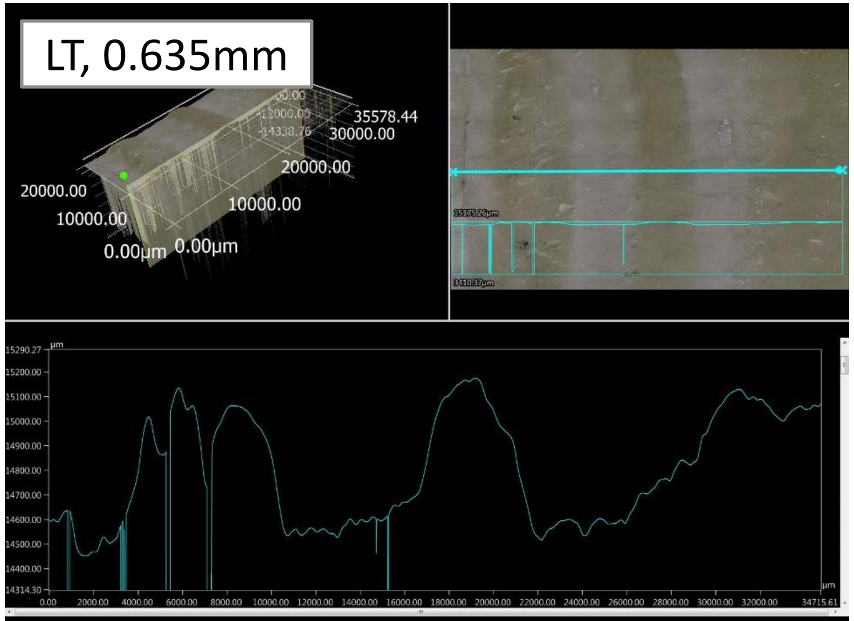

Rz: 646µm

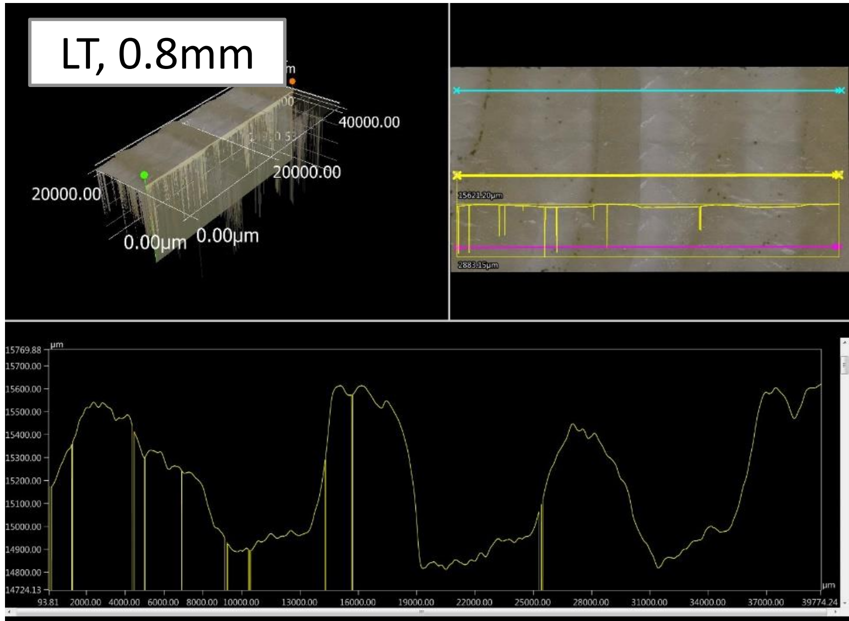

Rz: 681µm

Experimental Results – Mode-II

0.25mm

0.475mm

0.625mm

RT

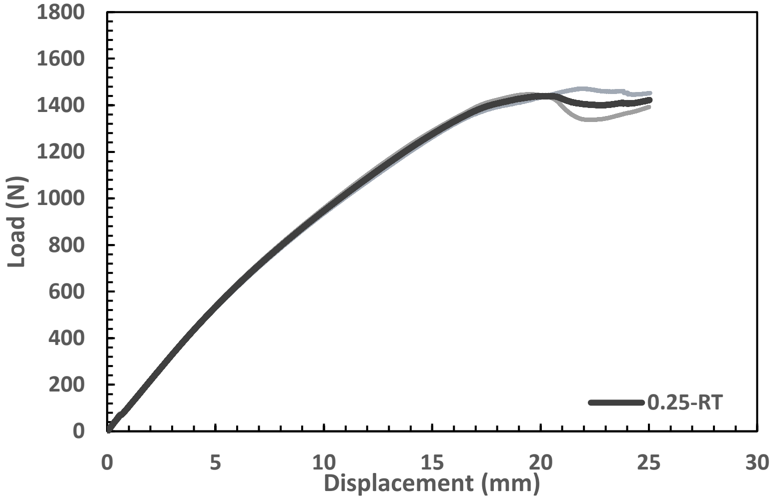

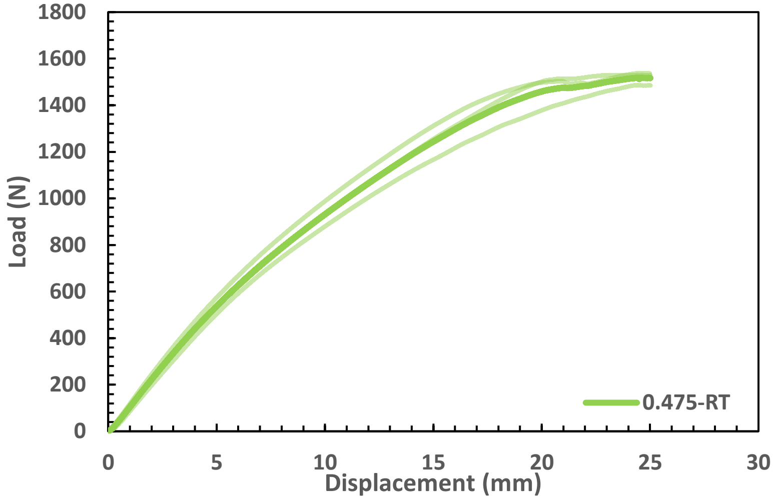

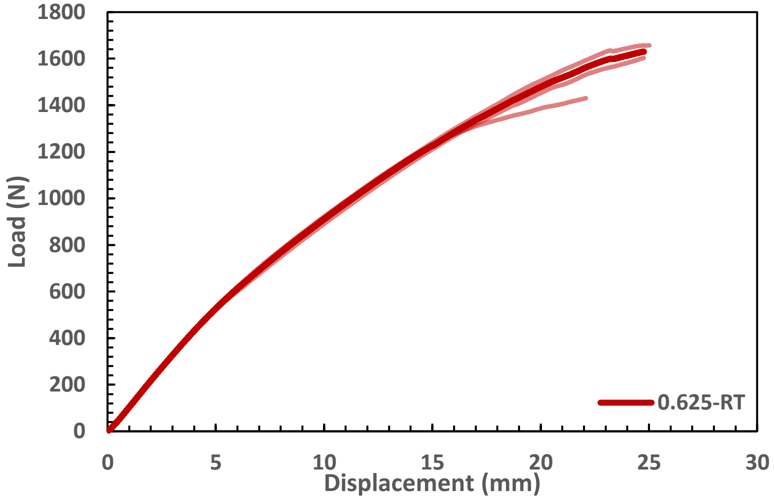

LT

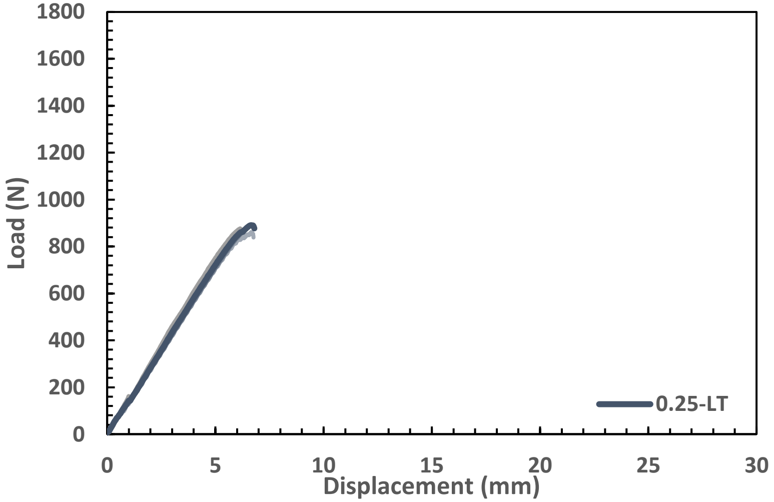

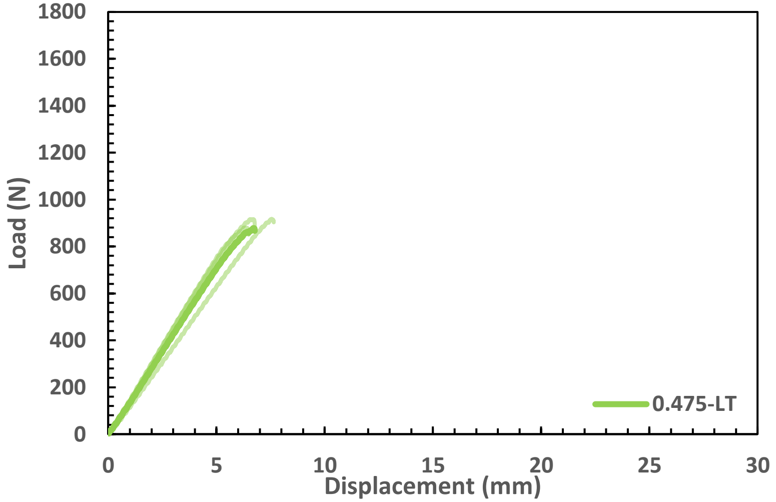

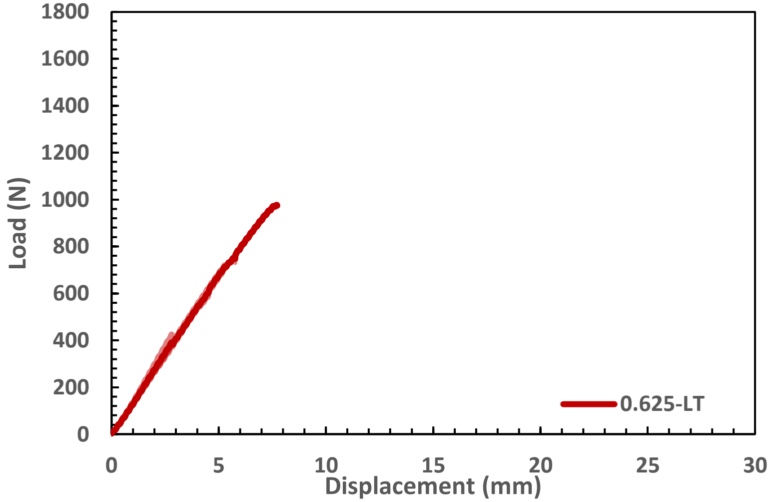

Experimental Results – Mode-II

- RT and LT G_{IIC} calculations incomplete due to challenges observing crack-tip during shear deformation
- Trials using DIC were unsuccessful for Mode-II crack tip tracking

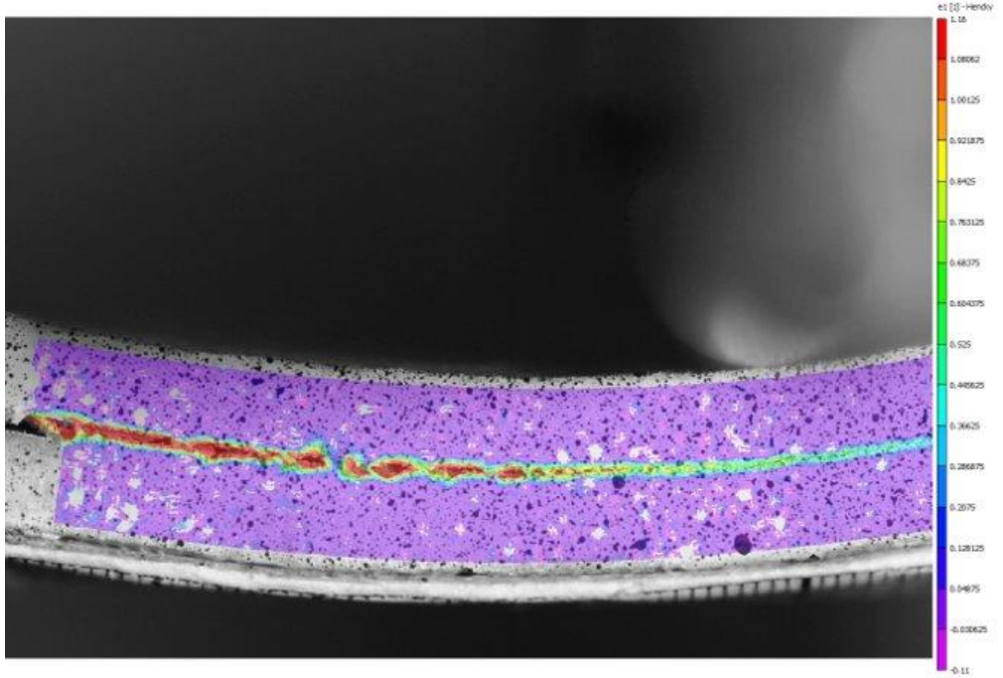

Unsuccessful DIC crack-tip monitoring trial.

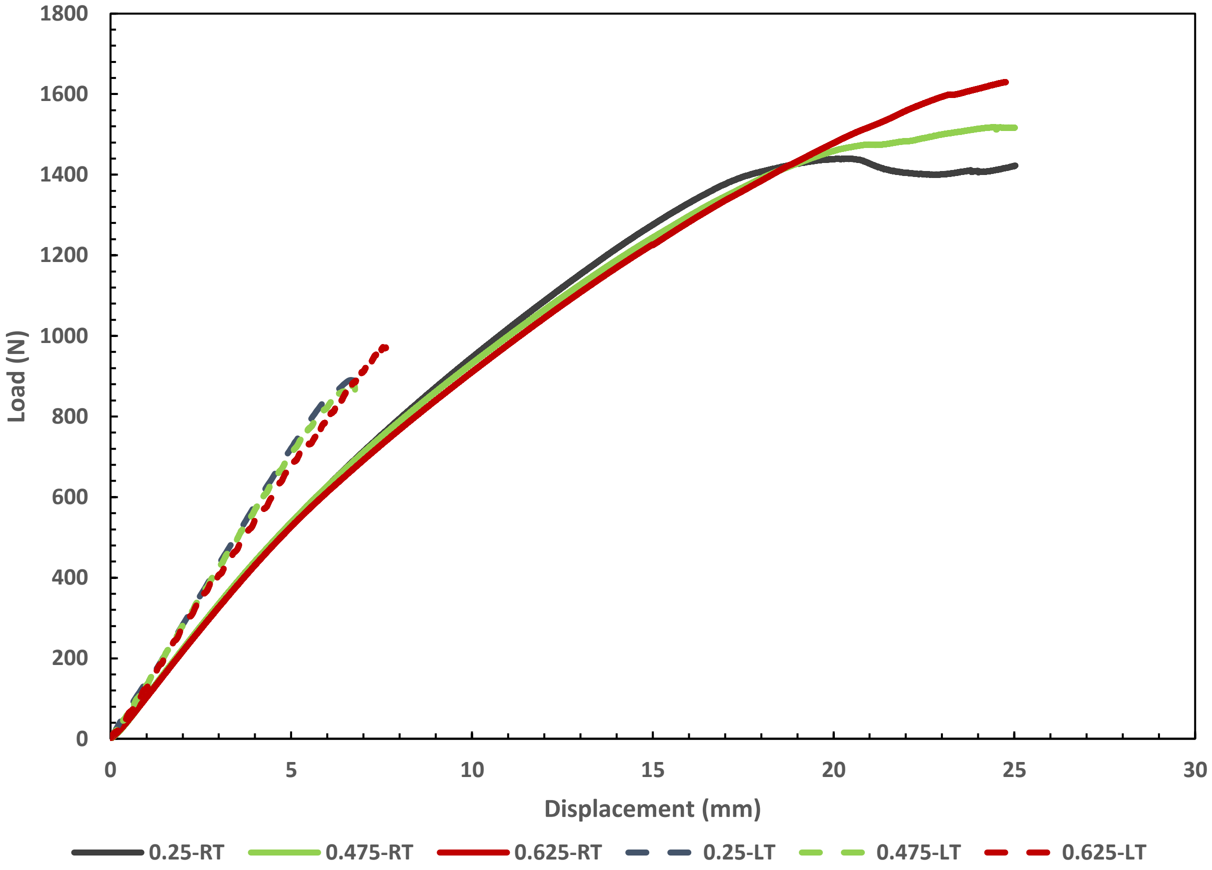

Overlay of average Load-Displacement curves for DCB tests at RT and LT.

Fracture Analysis – Mode-II RT

- RT-ENF specimens exhibit hackle formulations indicative of shear failure

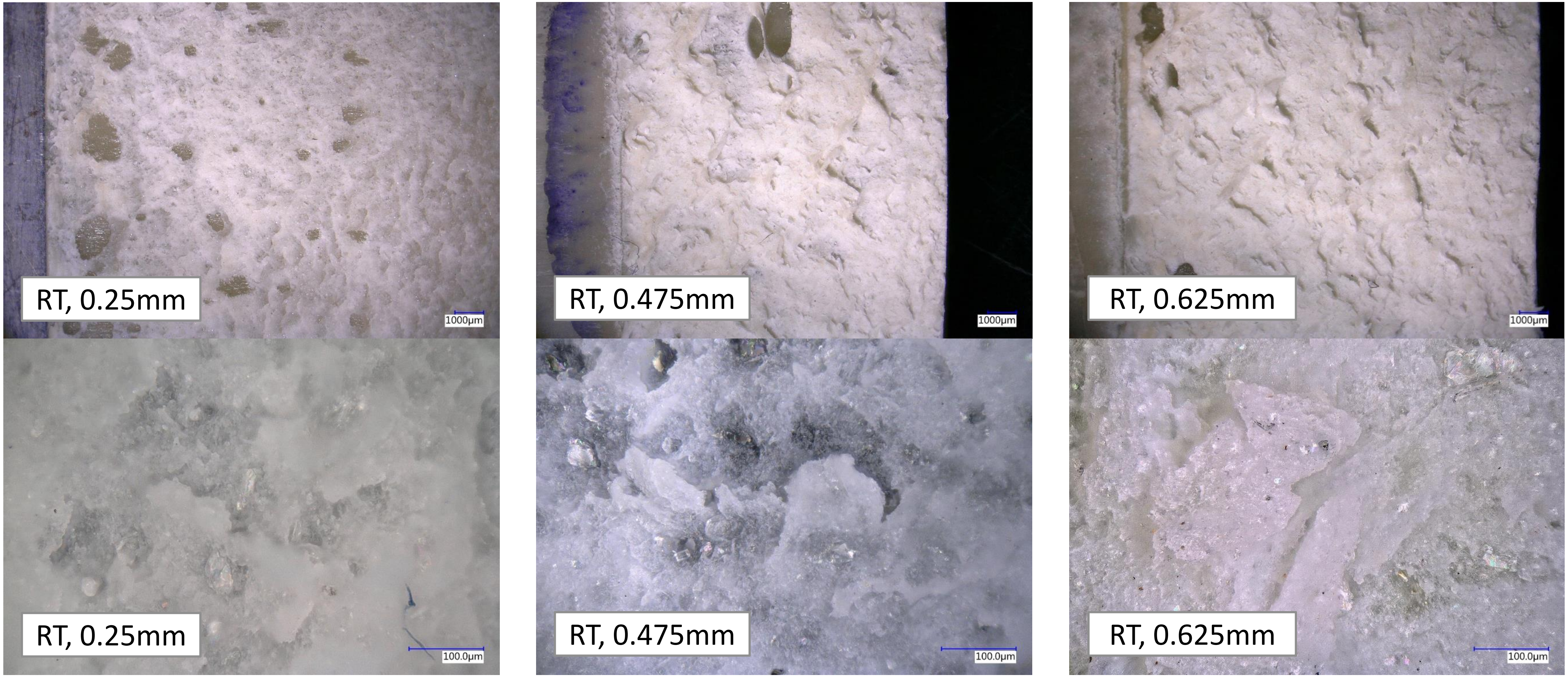

Fracture Analysis – Mode-II LT

- LT-ENF specimens experienced substrate failure (brittle deformation visible under microscope)

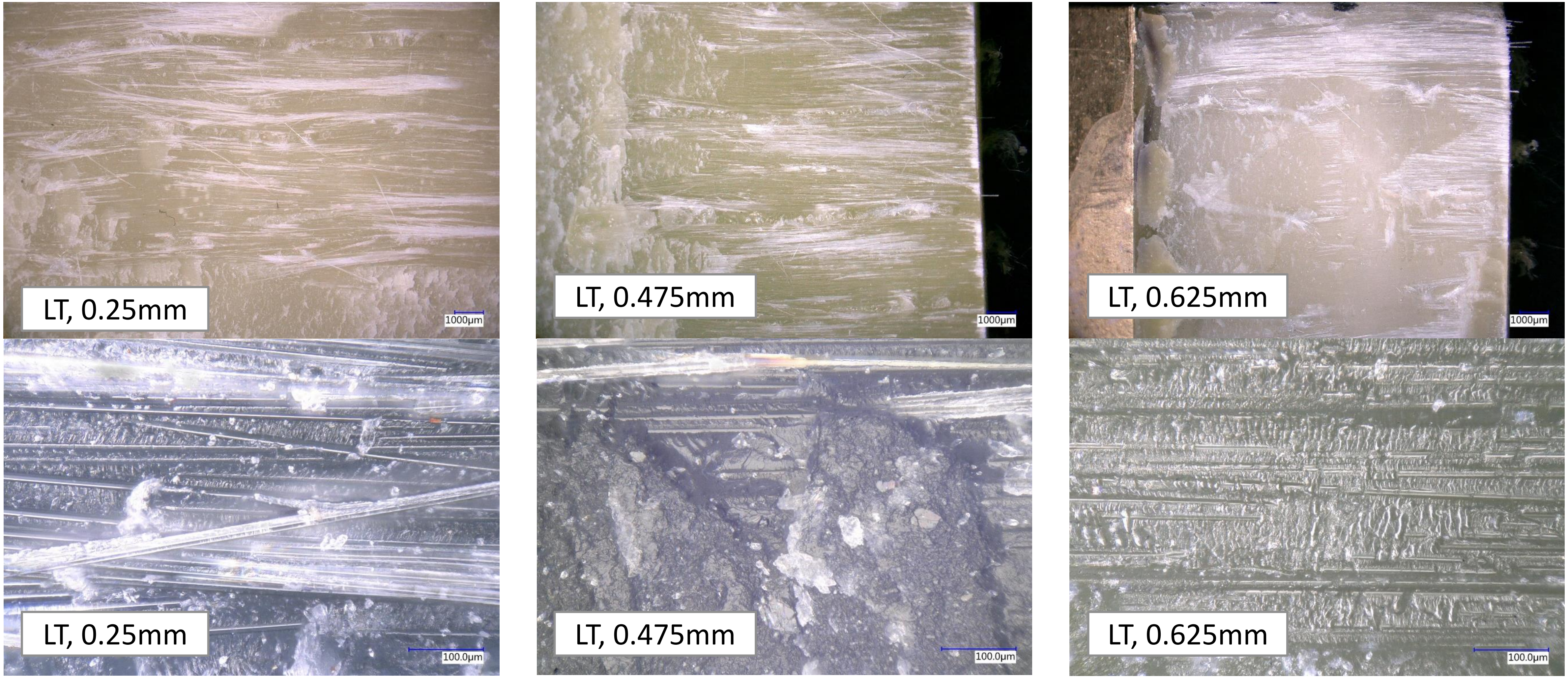

Conclusions and Next Steps

- **Key finding:** at extreme low temperatures (-40°C), the methacrylate adhesive experienced brittle cohesive failure during Mode-I testing and substrate failure during Mode-II testing.
- **At RT, peak load and displacement at failure increases with increasing bond-line thickness.**
- **At LT, primary modes of failure are combined brittle cohesive and interfacial failure (for each thickness).**
  - Varying coefficients of thermal expansion may contribute to stress concentrations within substrate (particularly around stitching sites).

- Obtaining G_{IC} for LT conditions requires performing additional LT-DCB tests.
- Determine G_{IIC} for RT and LT conditions using “effective” crack length method.
- Investigate influence of surface pretreatments on adhesive bond strength (e.g., laser etching and grit-blasting).

Acknowledgements

- Special thank you to Ramin Dehaghani and Mehdi Ghazimoradi (CRG) for assistance with vacuum infusion processes.
- Special thank you to Devon Hartlen (CRG) for assistance with lab training and specimen bonding.
- Special thank you to Professor Marco Alfano for feedback and input in adhesive bonding theory.

References

1. M. Quitoras, “Rethinking energy policy in Canada's remote communities,” Pembina Institute, 18-Nov-2020. [Online]. [Accessed: 04-May-2023].
2. R. E. Murray, J. Roadman, and R. Beach, “Fusion joining of thermoplastic composite wind turbine blades: Lap-shear bond characterization,” Renewable Energy, vol. 140, pp. 501–512, 2019.
3. Z. Jia, G. Yuan, D. Hui, X. Feng, and Y. Zou, “Effect of high loading rate and low temperature on mode I fracture toughness of ductile polyurethane adhesive,” Journal of Adhesion Science and Technology, vol. 33, no. 1, pp. 79–92, 2018.
4. R. Campilho, J. Ribeiro, R. Rocha, A. Leal, and F. Viana, “Validation of fracture envelopes of structural adhesives for mixed-mode strength prediction of bonded joints,” Frattura ed Integrità Strutturale, vol. 13, no. 48, pp. 332–347, 2019.
5. “ASTM D5528/D5528M-21 Standard Test Method for Mode I Interlaminar Fracture Toughness of Unidirectional Fiber-Reinforced Polymer Matrix Composites 1,” ASTM, vol. 15, no. 3, Jan. 2022.
6. B. Chen and D. A. Dillard, “The effect of the T-stress on crack path selection in adhesively bonded joints,” International Journal of Adhesion and Adhesives, vol. 21, no. 5, pp. 357–368, 2001.